

ORIGINAL RESEARCH

Overexpression of myocardin induces partial transdifferentiation of human-induced pluripotent stem cell-derived mesenchymal stem cells into cardiomyocytes

Jiao Zhang^{1,*}, Jenny Chung-Yee Ho^{1,2,*}, Yau-Chi Chan¹, Qizhou Lian^{1,2,3}, Chung-Wah Siu^{1,2} & Hung-Fat Tse^{1,2}

1 Division of Cardiology, Department of Medicine, Queen Mary Hospital, The University of Hong Kong, Hong Kong SAR, China

2 Research Centre of Heart, Brain, Hormone & Healthy Aging, Li Ka Shing Faculty of Medicine, The University of Hong Kong, Hong Kong SAR, China

3 Department of Ophthalmology, Li Ka Shing Faculty of Medicine, The University of Hong Kong, Hong Kong SAR, China

Keywords

Cardiomyocytes, mesenchymal stem cell, myocardin, transdifferentiation.

Correspondence

Hung-Fat Tse, Cardiology Division, Department of Medicine, The University of Hong Kong, Queen Mary Hospital, Hong Kong, China.

Tel: (852)-2255-4694

Fax: (852)-2818-6304

E-mail: hftse@hkucc.hku.hk

Funding Information

This study was supported by Small Project Funding (Project No. 201007176290 to J. C.-Y. H.); Hong Kong Research Grant Council General Research Fund (HKU 780110M and HKU 781111M to H.-F. T.); Hong Kong Research Grant Council Collaborative Research Fund (HKU8/CRF/09 to Q. L., C.-W. S., H.-F. T.); Theme-based Research Scheme (T12-705/11 to L. Q., C.-W. S., H.-F. T.); and Mr. Philip Wong Foundation Fund for Cardiac Stem Cell Research (H.-F. T.).

Received: 13 December 2013; Revised: 21 January 2014; Accepted: 26 January 2014

doi: 10.1002/phy2.237

Physiol Rep, 2 (2), 2014, e00237,
doi: 10.1002/phy2.237

*These authors contribute equally to this work.

Abstract

Mesenchymal stem cells (MSCs) derived from human-induced pluripotent stem cells (iPSCs) show superior proliferative capacity and therapeutic potential than those derived from bone marrow (BM). Ectopic expression of myocardin further improved the therapeutic potential of BM-MSCs in a mouse model of myocardial infarction. The aim was of this study was to assess whether forced myocardin expression in iPSC-MSCs could further enhance their transdifferentiation to cardiomyocytes and improve their electrophysiological properties for cardiac regeneration. Myocardin was overexpressed in iPSC-MSCs using viral vectors (adenovirus or lentivirus). The expression of smooth muscle cell and cardiomyocyte markers, and ion channel genes was examined by reverse transcription-polymerase chain reaction (RT-PCR), immunofluorescence staining and patch clamp. The conduction velocity of the neonatal rat ventricular cardiomyocytes cocultured with iPSC-MSC monolayer was measured by multielectrode arrays recording plate. Myocardin induced the expression of α -MHC, GATA4, α -actinin, cardiac MHC, MYH11, calponin, and SM α -actin, but not cTnT, β -MHC, and MLC2v in iPSC-MSCs. Overexpression of myocardin in iPSC-MSC enhanced the expression of SCN9A and CACNA1C, but reduced that of KCa3.1 and Kir2.2 in iPSC-MSCs. Moreover, BK_{Ca}, I_{Kir}, I_{Cl}, I_{to} and I_{Na,TTX} were detected in iPSC-MSC with myocardin overexpression; while only BK_{Ca}, I_{Kir}, I_{Cl}, I_{KDR}, and I_{KCa} were noted in iPSC-MSC transfected with green fluorescence protein. Furthermore, the conduction velocity of iPSC-MSC was significantly increased after myocardin overexpression. Overexpression of myocardin in iPSC-MSCs resulted in partial transdifferentiation into cardiomyocytes phenotype and improved the electrical conduction during integration with mature cardiomyocytes.

Introduction

Myocardin was identified as a transcription coactivator of serum response factor in mouse (Wang et al. 2001). The human myocardin gene expresses three alternative spliced mRNA variants (Torrado et al. 2003) with the longest isoform predominantly found in the heart (Du et al. 2003). Myocardin draws intensive interests because it activates the cardiac gene expression and influences heart function. The knockdown of the myocardin gene reduces the expression of cardiac markers in *Xenopus* and chick embryos (Wang et al. 2001; Small et al. 2005; Chen et al. 2008). Myocardin-deficient adult mouse exhibits early onset of heart failure, dilated cardiomyopathy, and premature death within 1 week (Huang 2009) suggesting that myocardin is essential for the development of ventricular cardiomyocytes (Hoofnagle et al. 2011). Overexpression of myocardin induced the expression of various cardiac-specific markers, such as cardiac troponin T (cTnT), MLC2a, MLC2v, α -MHC, β -MHC, GATA4, and sarco/endoplasmic reticulum Ca^{2+} -ATPase 2a (SERCA2a) in human bone marrow (BM)-mesenchymal stem cells (MSCs) (van Tuyn et al. 2005). In addition, myocardin regulates the expression of multiple smooth muscle cell (SMC) differentiation-related genes, including the smooth muscle (SM) α -actin, SM22 α , and SM-calponin (Du et al. 2003; van Tuyn 2003; Wang and Wang 2003; Yoshida et al. 2003; van Tuyn et al. 2005).

Furthermore, overexpression of myocardin further improved the therapeutic potential of BM-MSCs in a mouse model of myocardial infarction (Grauss et al. 2008), though the underlying mechanism remains unclear. Our recent studies have suggested that MSCs derived from human-induced pluripotent stem cells (iPSCs) have more potent proliferative capacity and exhibit better therapeutic efficacy in tissue regeneration than BM-MSCs (Lian et al. 2010). The aim of this study was to elucidate the effects of myocardin overexpression on MSC transdifferentiation, electrophysiological properties, and cellular integration of human iPSC-MSCs with rat cardiomyocytes by examining the expression of cardiac marker genes and ion channel genes, and measuring their electrical conduction velocity. In order to obtain a thorough examination on the effect of forced myocardin expression, both lentiviral and adenoviral transduction systems were used in this study. To mimic the situation of pulsed overexpression of myocardin at the initial stage of transdifferentiation, the non-integration approach of adenoviral system was used to provide a transient forced expression of myocardin. However, the lentiviral system was used to examine the effects of a sustainable myocardin overexpression via genome integration approach.

Materials and Methods

Cell culture

Human iPSC-MSCs were derived from iPSCs (iMR90)-4 (Lian et al. 2010). Human BM-MSCs were purchased from the Lonza Walkersville, Inc. (Walkersville, MD). The cells were cultured as monolayers in DMEM (Thermo Scientific, Waltham, MA) supplemented with 10% fetal bovine serum (FBS) (Invitrogen, Carlsbad, CA), 5 ng/mL bFGF (Invitrogen), and 5 ng/mL EGF (Peprotech, Hamburg, Germany).

Quantitative real-time polymerase chain reactions

Total RNA was extracted from the human BM-MSCs, human iPSC-MSCs, human myocardin-overexpressing iPSC-MSCs, GFP-overexpressing iPSC-MSCs, or cardiomyocytes derived from the human iPSCs ([iMR90]-4) (Lee et al. 2011), and it underwent RT-PCR with various primers (Table 1) as detailed in our previous work (Zhang et al. 2012).

Electrophysiology

The expression of ion channels in iPSC-MSC_{LV}^{myo} and iPSC-MSC_{LV}^{GFP} was examined by patch clamp techniques as detailed in our previous work (Zhang et al. 2012). In brief, the trypsinized cells were first seeded onto the glass coverslips in a four-well plate. After a 30–45 min recovery period in the incubator, the cells were transferred into Tyrode's solution for patch clamp experiments. Using a HEKA EPC-10 patch clamp amplifier and the PULSE v8.77 software (HEKA Instruments Inc., Southboro, MA), standard whole-cell patch clamp recordings were performed at room temperature. The action potentials were recorded under the current (C)-clamp at 37°C. Then, 1.5 mm thin-walled borosilicate glass tubing (1.2 mm outer diameter, 0.69 mm internal diameter) (Sutter Instrument Co., Novato, CA) were used to prepare pipettes using a P-97 Flaming/Brown micropipette puller (Sutter Instrument Co. Novato, CA). The typical pipette resistances were 3–4 M Ω when filled with internal pipette solution. After membrane rupture, the resting membrane potential was recorded under C-clamp without a current input. The recorded membrane potentials were corrected for a liquid junction potential of +15.6 mV under room temperature, and +15.9 mV under 37°C. During the action potential recordings, the cells were held at 0 pA with 0.1–1 nA stimulation for 5 msec to elicit a response.

Table 1. Oligonucleotide sequences of primers used for RT-PCR.

Gene name	Accession no.	Forward primer (5'–3')	Reverse primer (5'–3')	Product size (bp)
Myocardin	NM_001146312	TTCAGAGGTAACACAGCCTCC	TGATCCTCTAGCGTCTGCT	132
GAPDH	NM_002046	CCATCTCCAGGAGCGAG	GCAGGAGGCATTGCTGAT	233
SERCA2 α	NM_001110140	AAGCTATGGGAGTGGTGGTG	GCAATGCAAATGAGGGAGAT	138
α -MHC	GI 191623	GATGCCCAGATGGCTGACTT	GGTCAGCATGGCCATGTCCT	275
β -MHC	NM_080728.2	GCCAAACCAACCTGTCCAAGTTC	TGCAAAGGCTCCAGGTCTGAGGGC	203
cTnT	NM_000364	AGCATCTATAACTTGGAGGCAGAG	TGGAGACTTTCTGGTTATCCTTG	112
GATA4	NM_008092	TCTCCCAGGAACATCAAACC	GTGTGAAGGGGTGAAAAGG	125
Mef2c	NM_001131005	ATCTGCCCTCAGTCAGTTGG	AGAAGGCAGGGAGAGATTTGA	73
Mlc2v	NM_010861	GACCCAGATCCAGGAGTTCA	AATTGGACCTGGAGCCTCTT	163
Cx40	NM_005266	CTGGGCTGGAAGAAGATCAG	TGTGCAGCTCTGGACTATGC	102
Cx43	NM_000165	ATGAGCAGTCTGCCTTTCGT	TCTGCTCAAGTGCATGTCC	249
Cx45	NM_005497	AGCAGACAAGAAGGCAGCTC	TTAGGTTTGGGTTGGCTCTG	165
SM22	AB209555	AACAGCCTGTACCCTGATGG	CGGTAGTGCCCATCATTCTT	239
MYH11	NM_001040113	GGAGGATGAGATCCTGGTCA	TTAGCCGCACTCCAGTTCT	182
KCNH1 (a.k.a. EAG1 or Kv10.1)	NM_172362	TGGATTTGCAAGCTGTCTG	GAGTCTTTGGTGCCTCTTGC	476
Clcn3	NM_173872	CATAGGTCAAGCAGAGGGTC	TATTTCCGCAGCAACAGG	293
KCa1.1	U11058	ACAACATCTCCCCAACCC	TCATCACCTTCTTCCAATTC	310
KCa3.1	NM_002250	CGGGAACAAGTGAATCCAT	ACTGGGGAAGTAGCCTGTG	239
CACNA1C	NM_199460	AACATCAACAACGCCAACAA	AGGGCAGGACTGTCTTCTGA	574
Kir2.1	NM_000891	AACAGGGAGGTGTGGACAAG	TAACCTGCTTAGGGCTCCA	261
Kir2.2	NM_021012	GAGGCTATCACAGGCTCAGG	CCCCAAGTAAAAACCAGCA	183
Kir2.3	NM_152868	GCTTTGAGCCTGTGGTCTTC	TTGGCTCTGCTCTGAGTGTG	480
Kv1.4	NM_002233	ACGAGGGCTTTGTGAGAGAA	CACGATGAAGAAGGGGTCAT	308
Kv4.2	NM_012281	GCTTGTCATCAATCCCCTTG	TCCAGTATCTGGGCTTTTCC	102
Kv4.3	NM_172198	ACGGAGACATGGTGCCTAAG	CCCTGCGTTTATCAGCTCTC	153
SCN9A	NM_002977	GCTCCGAGTCTTCAAGTTGG	GGTTGTTGCATCAGGGTCT	446

Adenovirus preparation

The human myocardin gene (NM_001146312.1) was first amplified via PCR from human cardiac cDNA and ligated into the pCR2.1-TOPO shuttle vector (Invitrogen, Carlsbad, CA). The ORF was subsequently subcloned into pAD-shuttle-IRES-GFP (Stratagene, La Jolla, CA) for adenovirus production. Myocardin- and GFP-expressing adenoviruses were produced using the AdEasy™ XL Adenoviral Vector System (Stratagene, La Jolla, CA). The generated adenoviruses were purified using an Adeno Mini Purification ViraKit (Virapur LLC, SD, CA) before iPSC-MSCs transduction.

Lentivirus production and transduction

Myocardin or GFP gene was inserted into lentivirus expression vector pSIN-EF2-Pur (Addgene, MA), and cotransfected with pCMV-dR8.91 and pMD2G plasmid into 293FT cells (Invitrogen, Carlsbad, CA) using Lipofectamine 2000. Lentivirus were collected 3 days post transfection, filtered (0.45 μ m), and used to transduce iPSC-MSCs with polybrene (Millipore, Billerica, MA).

The positively transduced cells were selected using 0.5 μ g/mL puromycin-containing medium after 3 days post transduction.

Immunofluorescence staining

Cells seeded onto glass coverslips were washed with PBS, and fixed with 2% formalin for 30 min at room temperature. The cells were then incubated overnight with primary antibodies (1:200 dilutions in PBS) at 4°C. The primary antibodies included goat polyclonal anti-myocardin (Santa Cruz Biotechnology Inc., Santa Cruz, CA), mouse antihuman CD29 (Stemgent, San Diego, CA), mouse monoclonal anti- α -actinin (sarcomeric) (Sigma-Aldrich, Inc., St. Louis, MO), mouse anti-myosin heavy chain (cardiac) (Upstate Biotechnology Inc., Waltham, MA), mouse monoclonal antihuman α -actin (smooth muscle) (Dako, Copenhagen, Denmark), mouse monoclonal anti-troponin T (cardiac) (Thermo Scientific), and rabbit monoclonal anti-calponin-1 (Millipore, Billerica, MA). After washing twice with PBS, the cells were incubated with the secondary antibodies for 30 min at 4°C. The secondary antibodies consisted of Alexa-594 labeled rabbit anti-goat

IgG and Alexa-647 labeled rabbit anti-mouse IgG or Alexa-594 labeled donkey anti-goat IgG and Alexa-647 labeled donkey anti-rabbit IgG for myocardin and calponin co-staining. After washing twice, the cells were mounted onto glass slides with mounting medium containing 4',6-diamidino-2-phenylindole dihydrochloride (DAPI) (Invitrogen). Immunocomplex was examined by fluorescent microscopy (Olympus IX81). To facilitate overlaying multicolored imaging, Alexa 647 was switched to a virtual color of green (512 nm) using Xcellence Pro version 1.1 software.

Neonatal rat cardiomyocytes isolation and multielectrode arrays recording

In order to obtain viable cardiomyocyte to assess the electric conductance of the iPSC-MSCs, cardiomyocyte were isolated from neonatal rat hearts. The animal study protocol conforms to the Guide for the Care and Use of Laboratory Animals published by the United States National Institutes of Health and was approved by the ethics committee of the University of Hong Kong (1851-09). Hearts of neonatal Sprague-Dawley rats (0–2 days old) were dissected and rinsed with modified Hanks' balanced salt solution (Invitrogen, Carlsbad, CA) (supplemented with 0.81 mmol/L MgSO₄, 20 mmol/L HEPES, 100 U/mL penicillin and 100 µg/mL streptomycin, pH = 7.5 by NaOH). The ventricles were minced on ice and dissociated with 0.2% Trypsin 250 (BD Biosciences, San Jose, CA). The dissociated cells were centrifuged down and resuspended in prewarmed neonatal rat ventricular cardiomyocytes (NRVM) culture medium containing DMEM supplemented with 5% FBS, 100 U/mL penicillin, 100 µg/mL streptomycin, 1.5 mmol/L vitamin B₁₂ (Sigma-Aldrich), 10 mg/mL insulin (Sigma-Aldrich), 10 mg/mL transferrin (Sigma-Aldrich), and 0.1 mmol/L bromodeoxyuridine (Sigma-Aldrich). The cells were then filtered (70 µm), and preplated onto a 10-cm plate for exactly 1 h at 37°C.

The freshly isolated NRVMs were harvested, and mixed with myocardin- or GFP-overexpressing iPSC-MSCs at a ratio of 4:1, and seeded onto gelatin-coated multielectrode arrays (MEA) plates (Multi Channel Systems, Reutlingen, Germany) at approximately 10⁵ cells in total. The MEA plates used in this study contained 60 titanium nitride electrodes with a 200 µm interelectrode distance and 30 µm electrode diameter. The MEA plates combined with their supporting hardware allowed the simultaneous recording of extracellular electrical signals from all electrodes with one electrode as the ground. After allowing the NRVMs to settle down overnight, the electrical signals of the cell mixture were recorded and analyzed using the Cardio 2D+ software (Version 1.0.0) (Multi Channel Systems, Reutlingen, Germany).

Statistical analysis

The numeric data are presented as mean ± SEM. The statistical significance of the differences between group means was evaluated using analysis of variance (ANOVA) with post hoc Bonferroni test as appropriate. Differences with *P* < 0.05 were considered statistically significant.

Results

Myocardin overexpression in human iPSC-MSCs via lentivirus and adenovirus-mediated transfer

Positively transduced cells (i.e., iPSC-MSC_{LV}^{myo}, iPSC-MSC_{LV}^{GFP}, iPSC-MSC_{AD}^{myo}, iPSC-MSC_{AD}^{GFP}) were verified by RT-PCR and immunofluorescence staining. As shown in Figure 1A, the mRNA expression level of myocardin was significantly higher in iPSC-MSC_{LV}^{myo} and iPSC-MSC_{AD}^{myo} than in their corresponding GFP controls. Quantitative RT-PCR data revealed that the myocardin expression was 125- and 45-fold higher after lentivirus and adenovirus-mediated transfer, respectively, than the nontransduced cells (Fig. 1B). The myocardin protein was detected in the nucleus of iPSC-MSC_{LV}^{myo} and iPSC-MSC_{AD}^{myo}, but not in their GFP controls (Fig. 2). Lentivirus transduced cells were selected with puromycin before further experiments.

Overexpression of myocardin activated cardiomyocytes and smooth muscle cells marker genes of human iPSC-MSCs

The expression of the cardiac marker genes, including α-MHC and GATA4, was observed in myocardin-transduced human iPSC-MSCs, although lower than that of the cardiomyocyte control (Fig. 1). The expression level of SERCA, SM22, and connexin43 (Cx43) did not demonstrate obvious changes upon myocardin transduction. Mef2c was significantly upregulated upon myocardin transduction (2.7-fold) while the expression of connexin40 (Cx40) and connexin45 (Cx45) were downregulated in iPSC-MSC_{LV}^{myo} and iPSC-MSC_{AD}^{myo} (all *P* < 0.05, Fig. 1B). Moreover, there was no detectable expression of cTnT, β-MHC, and MLC2v in iPSC-MSC_{LV}^{myo} and iPSC-MSC_{AD}^{myo}. On the other hand, iPSC-MSC_{LV}^{myo} activated the expression of the SMC marker gene MYH11. Figure 2 illustrates the positive staining for calponin, SM α-actin, α-actinin, and cardiac MHC, along with myocardin, in iPSC-MSC_{AD}^{myo} and iPSC-MSC_{LV}^{myo}, but not in iPSC-MSC_{AD}^{GFP}, iPSC-MSC_{LV}^{GFP}, iPSC-MSCs, or BM-MSCs.

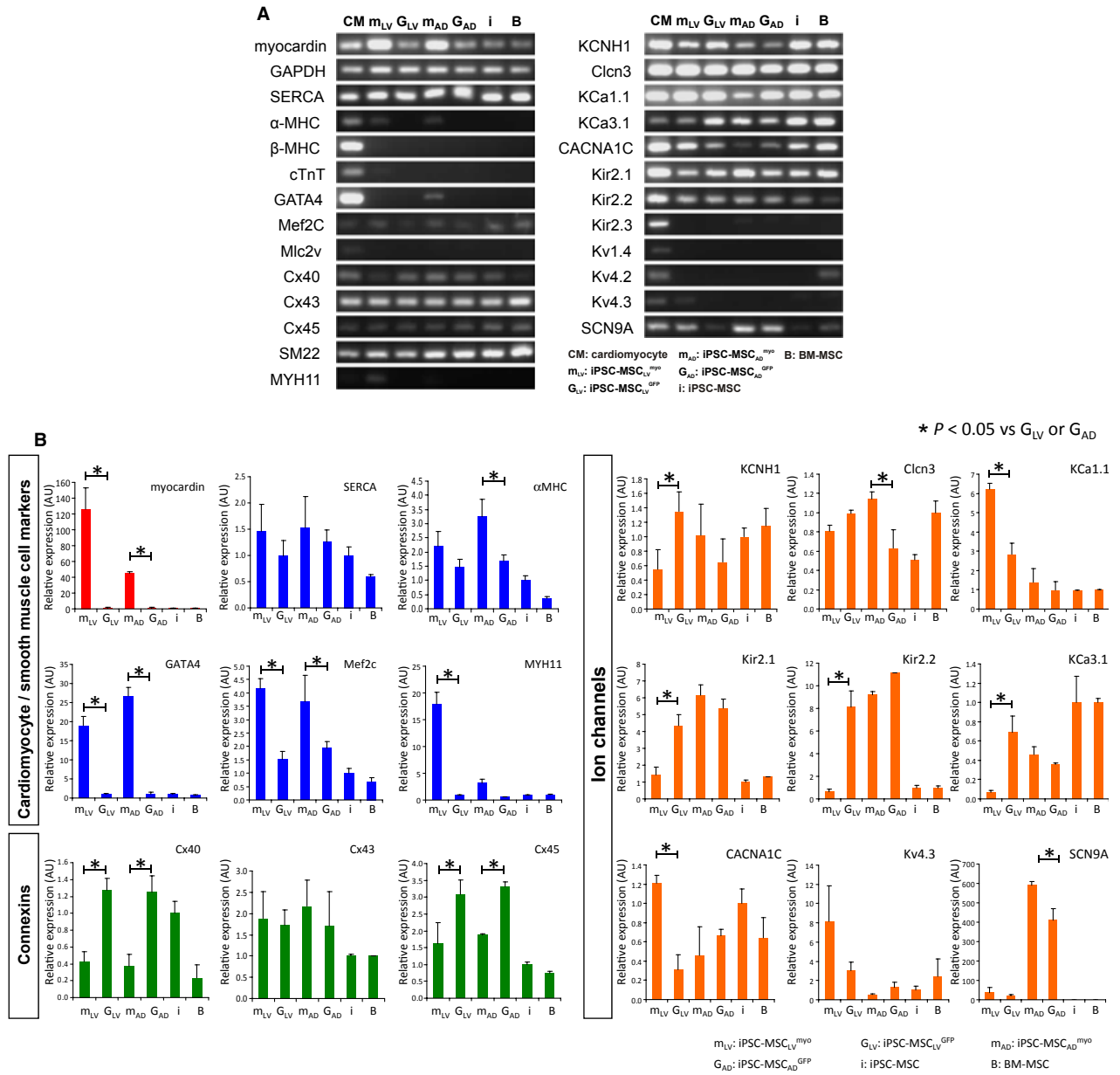


Figure 1. Gene expression analysis of myocardin expressing iPSC-MSC. (A) Results of RT-PCR for the detection of cardiomyocyte, smooth muscle cell marker genes, and ion channels genes expression. qPCR data are presented as relative fold change with reference to BM-MSC. (B) Quantitative real-time polymerase chain reaction (q-PCR) gene expression analysis of myocardin expressing iPSC-MSC. Relative expression cardiomyocyte, smooth muscle cell marker genes, connexins, and ion channels genes expression with reference to iPSC-MSC are presented. No detectable expression MHC, cTnT, Mlc2v, Kir2.3, Kv1.4, and Kv4.2 were found in iPSC-MSC. *P < 0.05 versus G_{LV} or G_{AD}, respectively.

Overexpression of myocardin-modulated ion channel profile of human iPSC-MSCs

According to the RT-PCR results (Fig. 1), the expression of Kv4.3 (responsible for I_{to}) (2.2-fold), SCN9A (for I_{Na,TTX}) (1.9-fold), and CACNA1C (for I_{Ca,L}) (3.9-fold) were upregulated, whereas the expression of KCNH1 (for I_{KDR}) (2.5-fold), KCa3.1 (for I_{KCa}) (9.9-fold), Kir2.1 and

Kir2.2 (for I_{Kir}) (3.1- and 13.1-fold, respectively) were downregulated in iPSC-MSC_{LV}^{myo} compared with that in iPSC-MSC_{LV}^{GFP} (all P < 0.05). No significant difference in the expression of Clcn3 (for I_{Cl}) was observed between iPSC-MSC_{LV}^{myo} and iPSC-MSC_{LV}^{GFP}.

The functional expression of the ion channels was then further examined by patch clamp in iPSC-MSC_{LV}^{myo} (n = 282) and iPSC-MSC_{LV}^{GFP} (n = 101). Lentivirus-

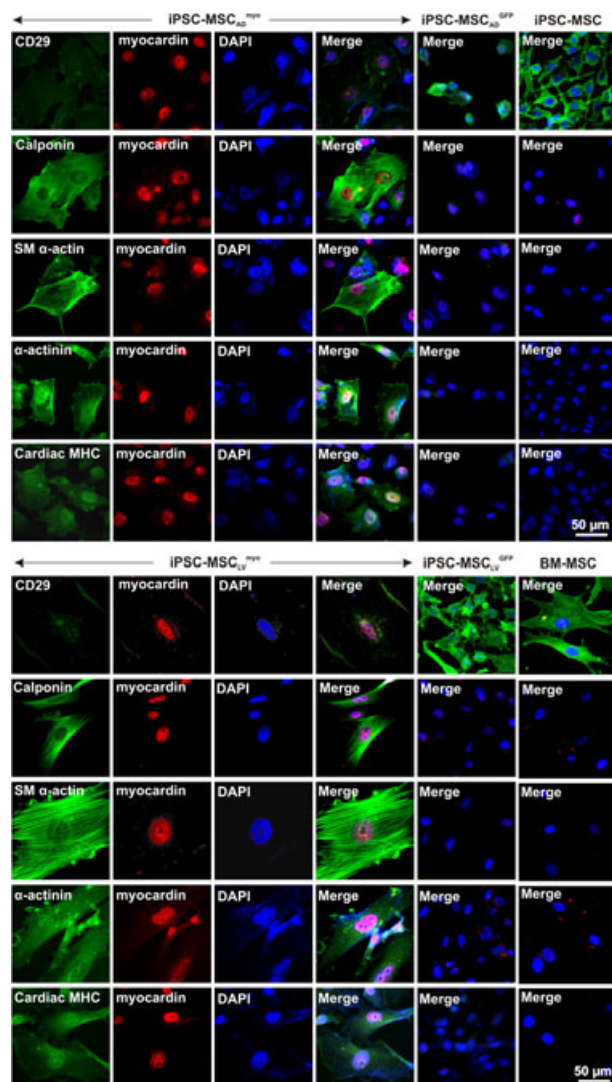


Figure 2. Immunofluorescence staining of myocardin with cardiomyocyte or smooth muscle cell marker genes as depicted in the figure. Adenovirus-transduced samples were fixed 3 days post transduction, lentivirus transduced cells were fixed 12–14 days post transduction.

mediated transduction combined with puromycin selection was adopted to ensure the successful transduction of myocardin or GFP in each cell for patch clamp. A current, likely I_{Cl} (Tao et al. 2007), was recorded in 26% of iPSC-MSC_{LV}^{myo} (72 of 282) and 3% of iPSC-MSC_{LV}^{GFP} (3 of 101) as shown in Figure 3. The identity of I_{Cl} was confirmed using a chloride channel blocker DIDS. The current was inhibited by DIDS (150 μ mol/L) in a representative iPSC-MSC_{LV}^{myo} (Fig. 3A) or iPSC-MSC_{LV}^{GFP} (Fig. 3B). Figure 3A lower panel illustrates the I–V relationship curve of the DIDS-sensitive current in iPSC-MSC_{LV}^{myo} ($n = 7$), by subtracting currents recorded after

DIDS administration from the control current accordingly.

This inward component exhibited properties similar to I_{Kir} (Deng et al. 2006) were observed in both iPSC-MSC_{LV}^{myo} (9%, 18 of 282) and iPSC-MSC_{LV}^{GFP} (12%, 11 of 101). The existence of I_{Kir} was determined using 0.5 mmol/L Ba²⁺, a specific blocker for I_{Kir} . As displayed in Figure 4A and B, the inward rectifying K⁺ current was reversibly suppressed by 0.5 mmol/L BaCl₂ in both iPSC-MSC_{LV}^{myo} and iPSC-MSC_{LV}^{GFP}. The I–V relationships of I_{Kir} , elicited with a 1.2 sec ramp protocol (from -120 to 0 mV) in a solution containing 5 mmol/L K⁺ (Tyrode's solution) or 20 mmol/L K⁺, and after application of 0.5 mmol/L Ba²⁺ in the bath solution are illustrated in a representative iPSC-MSC_{LV}^{myo} (Fig. 4A, lower panel) or iPSC-MSC_{LV}^{GFP} (Fig. 4B, lower panel). Similar results were observed in 12 iPSC-MSC_{LV}^{myo} and 4 iPSC-MSC_{LV}^{GFP}.

An outward current, likely BK_{Ca} current (Li et al. 2005), was activated in both iPSC-MSC_{LV}^{myo} (68%, 191 of 282) and iPSC-MSC_{LV}^{GFP} (85%, 86 of 101) as shown in Figure 5A and B. The identity of BK_{Ca} was confirmed using the BK_{Ca} channel-specific blocker paxilline (Fig. 5A and B). After administration of paxilline, the current activated at +60 mV, was significantly reduced from 2.9 ± 0.4 pA/pF to 1.0 ± 0.12 pA/pF in iPSC-MSC_{LV}^{myo} ($n = 11$, $P < 0.001$), and from 28.6 ± 8.4 pA/pF to 8.6 ± 1.9 pA/pF in iPSC-MSC_{LV}^{GFP} ($n = 9$, $P < 0.05$).

Two types of paxilline-resistant currents were recorded in iPSC-MSC_{LV}^{GFP} but not in iPSC-MSC_{LV}^{myo}. As shown in Figure 5C, a paxilline-resistant current in a representative iPSC-MSC_{LV}^{GFP} was further inhibited by IK_{DR} blocker 4-AP. Paxilline (1 μ mol/L) partially suppressed the membrane current at +60 mV from 19.2 ± 3.7 pA/pF to 9.2 ± 2.4 pA/pF. The remaining current was inhibited by 4-AP (5 mmol/L) to 2.2 ± 1.5 pA/pF ($n = 5$, $P < 0.05$). The other type of current displayed properties of IK_{Ca} (Tao et al. 2007) was detected only in iPSC-MSC_{LV}^{GFP} (6%, 6 of 101). In Figure 5D, the outward current in a representative iPSC-MSC_{LV}^{GFP} was partially inhibited by paxilline (1 μ mol/L), with the remaining current completely blocked by the IK_{Ca} blocker clotrimazole (1 μ mol/L). Similar results were observed in five iPSC-MSC_{LV}^{GFP} cells.

Two other types of currents were recorded in iPSC-MSC_{LV}^{myo} but not in iPSC-MSC_{LV}^{GFP}. One was the transient outward K⁺ current I_{to} sensitive to 4-AP (Li et al. 2005). I_{to} was detected in a small portion of iPSC-MSC_{LV}^{myo} (4%, 11 of 282) with a representative one shown in Figure 6A. The voltage-dependent inactivation of I_{to} was assessed by the step potential at +50 mV after 1000 ms conditioning potentials from -110 to 0 mV (Fig. 6B). The I_{to} inactivation curve was obtained by

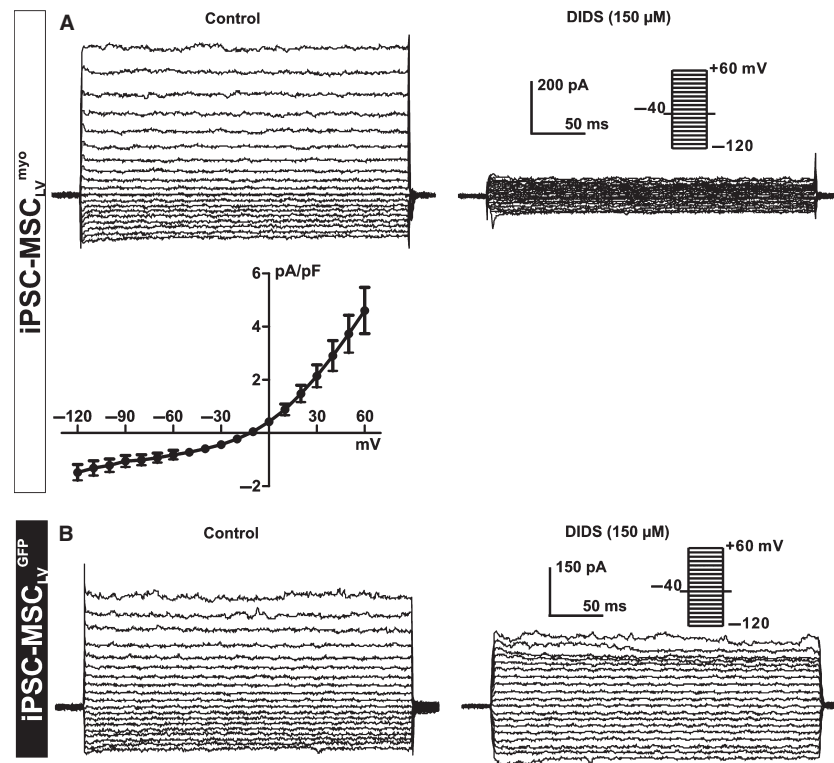


Figure 3. I_{Cl} in iPSC-MSC_{LV}^{myo} and iPSC-MSC_{LV}^{GFP}. Voltage-dependent current was inhibited by the Cl^- channel blocker DIDS (150 μ mol/L) in a representative iPSC-MSC_{LV}^{myo} (A) or iPSC-MSC_{LV}^{GFP} (B). Current was elicited by the protocol shown in the inset. I–V relationship of DIDS-sensitive current obtained by subtracting the currents recorded before and after DIDS application in iPSC-MSC_{LV}^{myo} ($n = 7$) (A, lower panel).

plotting I/I_{max} of I_{to} (the peak value of I_{to} normalized to the maximum one) as a function of the conditioning potentials and fitting to the Boltzmann sigmoidal curve. The slope of the I_{to} inactivation curve was approximately 9.3 ± 1.7 , and the half inactivated conditioning potential was approximately -64.0 ± 1.9 mV ($n = 6$). The time-dependent recovery of I_{to} from inactivation was estimated with a paired-pulse protocol (shown in the inset of Fig. 6C). The I_{to} recovery curve was fit to an exponential function-one phase association with the time constant (ζ) 61.5 msec and half-time 42.6 msec ($n = 4$).

The other current exclusively observed in iPSC-MSC_{LV}^{myo} was an inward current activated from approximately -30 to $+60$ mV and sensitive to tetrodotoxin (TTX). This phenomenon suggested the existence of $I_{Na,TTX}$ (Li et al. 2005) in iPSC-MSC_{LV}^{myo} (4%, 12 of 282). Figure 6D demonstrates that TTX (100 nmol/L) reversibly inhibited the inward current, with limited effects on the outward current. Similar results were observed in four iPSC-MSC_{LV}^{myo} cells.

In summary, a similar functional ion channel profile (i.e., BK_{Ca} , I_{Kir} , I_{Cl} , IK_{DR} , and IK_{Ca}) as in iPSC-MSCs (Zhang et al. 2012) was observed in iPSC-MSC_{LV}^{GFP} (85%,

12%, 3%, 56%, and 6%). Two distinct ion channels, I_{to} and $I_{Na,TTX}$ were recorded in iPSC-MSC_{LV}^{myo} (68%, 9%, 26%, 4%, and 4%).

Furthermore, iPSC-MSC_{LV}^{myo} had a RMP of -25.9 ± 0.7 mV, which was more depolarizing than that of iPSC-MSC_{LV}^{GFP} (-32.1 ± 1.6 mV) ($P < 0.001$). In addition, the cell size of iPSC-MSC_{LV}^{myo} was significantly increased upon myocardin transduction than iPSC-MSC_{LV}^{GFP} ($P < 0.001$), as reflected by their respective average membrane capacitance (69.3 ± 2.5 pF vs. 22.4 ± 1.7 pF).

Myocardin overexpressed iPSC-MSCs did not exhibit action potentials as mature cardiomyocytes

To assess whether overexpression of myocardin resulted in complete cardiomyocyte differentiation of iPSC-MSCs, the action potential of iPSC-MSC_{LV}^{myo}, iPSC-MSC_{LV}^{myo} incubated in cardiomyocyte differentiation medium, iPSC-MSC_{AD}^{myo}, and their GFP controls ($n = 11–23$) were also characterized (Fig. 7). However, none of these cells exhibited action potentials as mature cardiomyocytes.

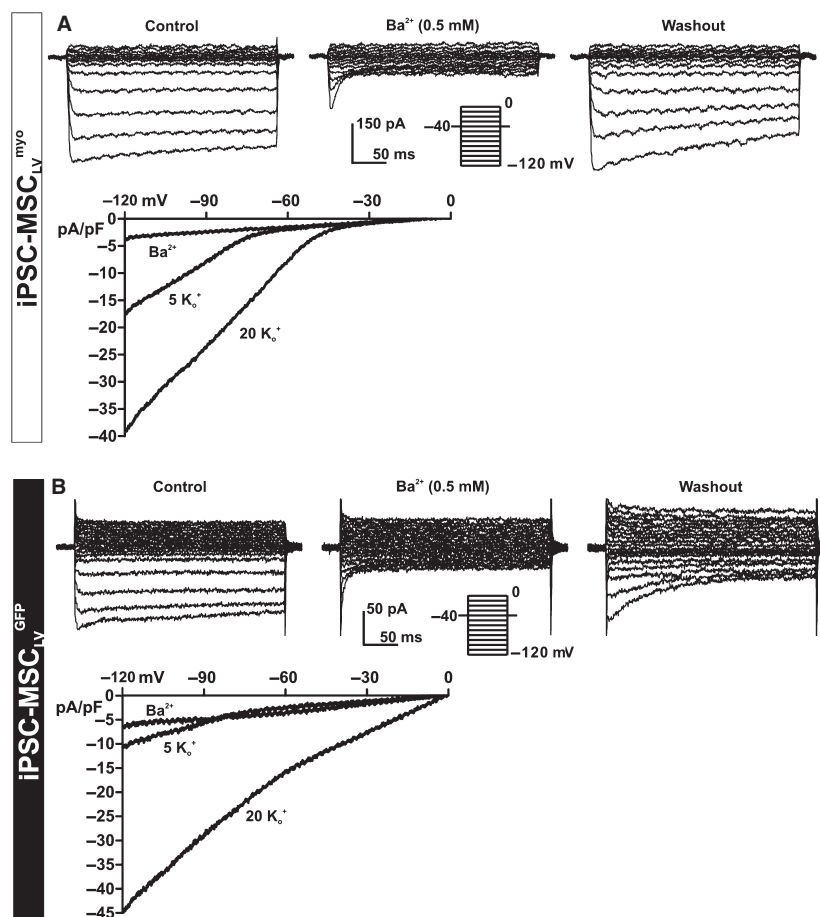


Figure 4. I_{Kir} in iPSC-MSC_{LV}^{myo} and iPSC-MSC_{LV}^{GFP}. Voltage-dependent currents, elicited with the inset protocol, were reversibly inhibited by BaCl₂ (0.5 mmol/L) in a representative iPSC-MSC_{LV}^{myo} (A) or iPSC-MSC_{LV}^{GFP} (B), or with a 1.2-sec ramp protocol (–120 to 0 mV from a holding potential of –40 mV) in another representative iPSC-MSC_{LV}^{myo} (A, lower panel) or iPSC-MSC_{LV}^{GFP} (B, lower panel) in the presence of 5 mmol/L K_o⁺, 20 mmol/L K_o⁺, or 0.5 mmol/L Ba²⁺ in bath solution.

Overexpression of myocardin significantly increased the electrical conduction velocity of human iPSC-MSCs

The effects of myocardin overexpression on the cellular integration and conductance changes of iPSC-MSC with cardiomyocytes were determined by measuring the electrical conduction velocity in a monolayer coculture of iPSC-MSC_{AD}^{myo} or iPSC-MSC_{AD}^{GFP} with NRVMs on MEA recording plates (Fig. 8A). The electrical signals transmitted through the MEA plate were recorded as shown in a representative iPSC-MSC_{AD}^{GFP} (Fig. 8B) or iPSC-MSC_{AD}^{myo} (Fig. 8C), coculture system. The electrical conduction velocities of iPSC-MSC_{AD}^{myo} ($n = 13$; 0.13 ± 0.03 m/sec) were significantly faster than those of iPSC-MSC_{AD}^{GFP} ($n = 15$; 0.07 ± 0.01 m/sec) (Fig. 8D, $P < 0.05$).

Discussion

Recent clinical studies have suggested that MSC is a potential cell source for cardiac regeneration in patients with myocardial infarction and heart failure (Siu and Tse 2012). The underlying mechanisms of the beneficial effect of MSC for cardiac regeneration likely mediated through multiple actions, including transdifferentiation into functional cardiomyocyte or fusion with native cardiomyocytes, paracrine effects, cell-cell interactions, and integration with native cardiomyocytes (Williams and Hare 2011). Previous studies have shown that myocardin activates cardiac gene expression in BM-MSCs (van Tuyn et al. 2005), and improved their therapeutic potential for myocardial infarction (Grauss et al. 2008).

This study is the first to investigate the effect of myocardin overexpression in human iPSC-MSCs. Our

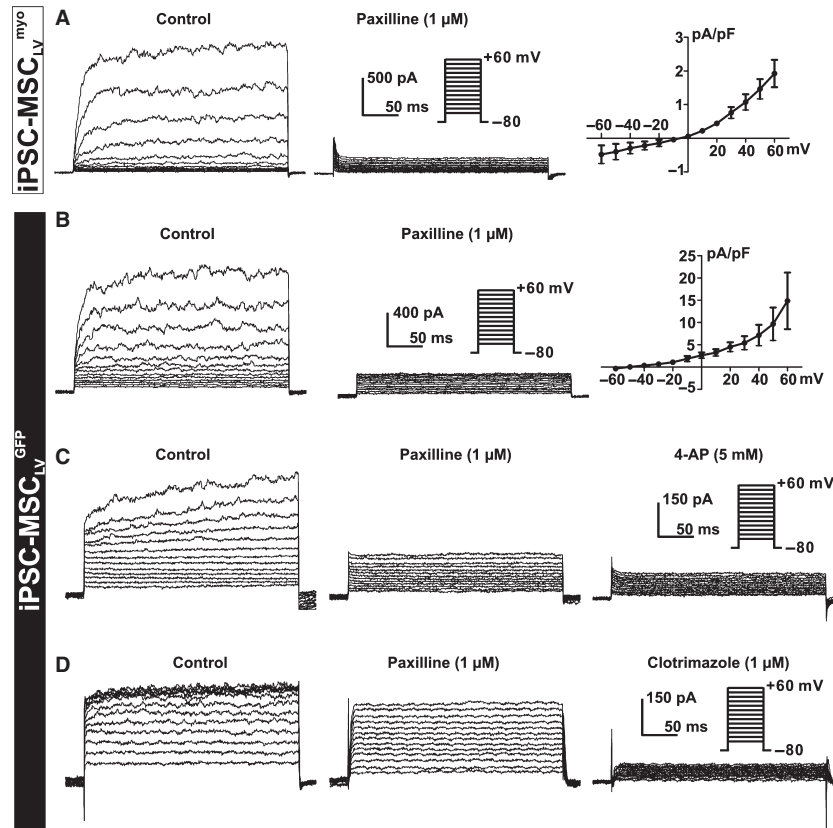


Figure 5. BK_{Ca} in $iPSC-MSC_{LV}^{myo}$, BK_{Ca} , IK_{DR} , and IK_{Ca} in $iPSC-MSC_{LV}^{GFP}$. Noisy currents were completely inhibited by paxilline ($1 \mu\text{mol/L}$) in a representative $iPSC-MSC_{LV}^{myo}$ (A) or $iPSC-MSC_{LV}^{GFP}$ (B). I-V relationship of paxilline-sensitive currents obtained by subtracting the currents before and after paxilline treatment accordingly in $iPSC-MSC_{LV}^{myo}$ ($n = 12$) (A, right panel) and $iPSC-MSC_{LV}^{GFP}$ ($n = 5$) (B, right panel). Voltage-dependent currents in a representative $iPSC-MSC_{LV}^{GFP}$ were partially inhibited by paxilline ($1 \mu\text{mol/L}$) and completely abolished by 4-AP (5 mmol/L) ($n = 5$) (C) or clotrimazole ($1 \mu\text{mol/L}$) ($n = 3$) (D). Currents were elicited by the protocol shown in the inset.

previous studies have shown that iPSC-MSCs exhibit higher proliferative potential and better therapeutic efficacy for tissue regeneration (Lian et al. 2010; Zhang et al. 2012). In this study, the myocardin overexpression in human iPSC-MSCs resulted in partial transdifferentiation into cardiomyocyte phenotypes as reflected by the appearance of cardiac markers α -MHC, GATA4, α -actinin, and cardiac MHC, but not cardiac markers cTnT, β -MHC, MLC2v, and cTnT protein. These findings were consistent with those observed in myocardin overexpression in BM-MSC (van Tuyn et al. 2005; Grauss et al. 2008). Therefore, myocardin overexpression alone could not induce complete cardiomyocyte transdifferentiation from iPSC-MSCs as observed in BM-MSC. The incomplete transdifferentiation into mature cardiomyocyte phenotypes from myocardin-transduced iPSC-MSCs was further confirmed by the lack of mature action potentials recorded by patch clamping (data not shown). It is likely that those phenotypic changes of the MSC are due to secondary effect of multiple genes expression induced by

myocardin rather than direct myocardin transcriptional activity to induce complete cardiac transdifferentiation. Moreover, our findings reveal several similar as well as different gene expression profiles related transient versus long-term expression of myocardin using adenovirus and lentivirus transduction, respectively.

In this study, we characterized and compared the ion channel profiles of $iPSC-MSC_{LV}^{myo}$ and $iPSC-MSC_{LV}^{GFP}$ to assess the electrophysiological effects of myocardin overexpression on iPSC-MSCs. RT-PCR results revealed that $iPSC-MSC_{LV}^{myo}$ has higher expression levels of $Kv4.3$ (responsible for I_{to}), $KCa1.1$ (for BK_{Ca}), $SCN9A$ (for $I_{Na,TTX}$), and $CACNA1C$ (for $I_{Ca,L}$), but lower expression levels of $KCa3.1$ (for IK_{Ca}), $KCNH1$ (for IK_{DR}), and $Kir2.1$ (for IK_{ir}) than those of $iPSC-MSC_{LV}^{GFP}$. Both $iPSC-MSC_{LV}^{myo}$ and $iPSC-MSC_{LV}^{GFP}$ had similar expression levels of $Clcn3$ (for I_{Cl}). Patch clamp results showed that BK_{Ca} , IK_{ir} , I_{Cl} , I_{to} , and $I_{Na,TTX}$ were expressed in $iPSC-MSC_{LV}^{myo}$ (68%, 9%, 26%, 4%, and 4%), compared with BK_{Ca} , IK_{ir} , I_{Cl} , IK_{DR} and IK_{Ca} in

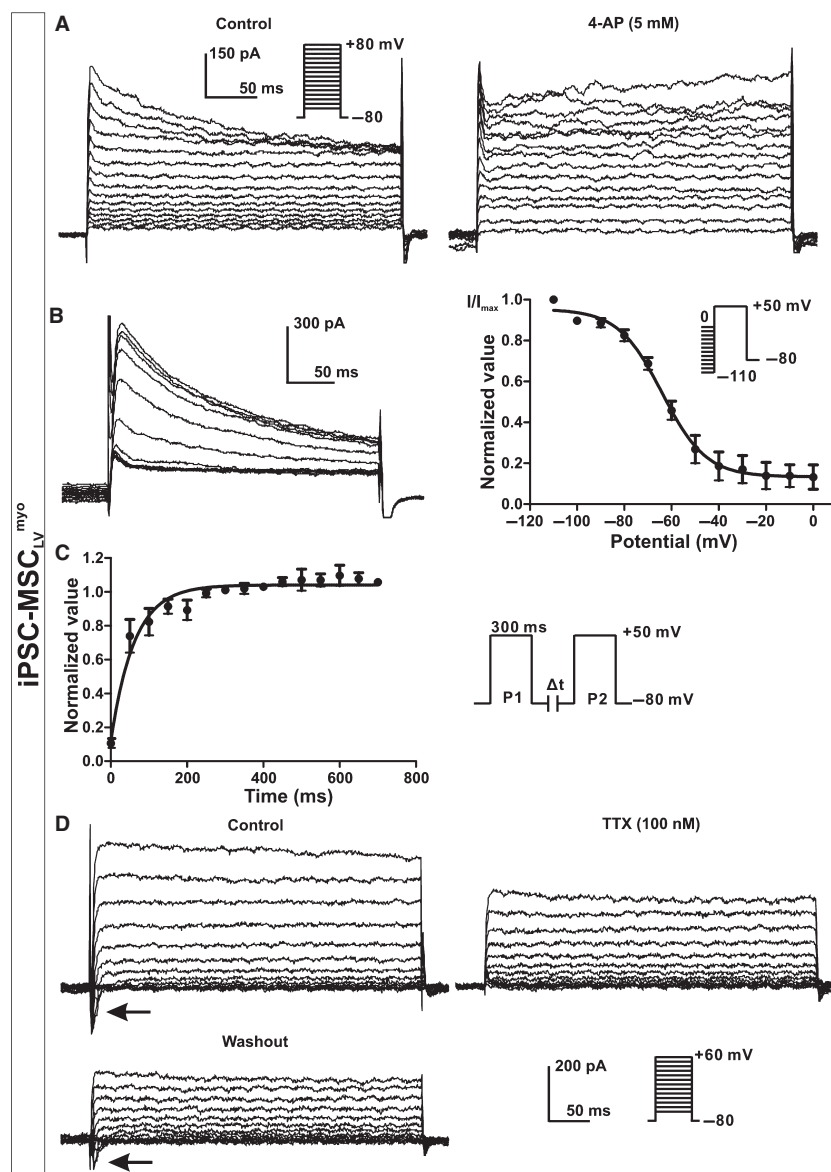


Figure 6. I_{to} and $I_{Na,TTX}$ in iPSC-MSC^{myo}. (A) I_{to} currents in a representative iPSC-MSC^{myo} were inhibited by 4-AP (5 mmol/L). (B) Voltage-dependent inactivation of I_{to} in a representative cell and normalized mean values (I/I_{max}) under different voltages ($n = 6$). (C) The recovery curve of I_{to} . P2 current was normalized by P1 current and plotted against the P1-P2 interval ($n = 5$). (D) An inward current (arrow) recorded in a representative cell was reversibly inhibited by TTX (100 nmol/L) ($n = 4$). Currents were elicited by the protocol shown in the inset.

iPSC-MSC^{LV}^{GFP} (85%, 12%, 3%, 56%, and 6%). Overexpression of myocardin upregulated the functional expression of I_{Cl} channels and activated the functional expression of I_{to} and $I_{Na,TTX}$ channels, but inhibited the functional expression of the I_{Ca} , I_{KDR} and I_{Kir} channels.

The expression of the human *Clcn3* gene is mainly found in the skeletal muscle and brain (Borsani et al. 1995). The inactivation of the *Clcn3* gene causes severe myocardial hypertrophy and heart failure in knockout mice (Xiong et al. 2010). *Clcn3* encodes the I_{Cl} channel,

which is volume-sensitive and can be activated under hypotonic conditions, as shown in human gastric epithelial cells (Jin et al. 2003), mouse BM-MSCs (Tao et al. 2007), and bovine epithelial cells (Wang et al. 2000). In this study, the size of the iPSC-MSC^{LV}^{myo} greatly expanded compared with iPSC-MSC^{LV}^{GFP}, as reflected by the increase in the average membrane capacitance from 22.4 ± 1.7 pF to 69.3 ± 2.5 pF. The percentage of cells that displayed I_{Cl} currents increased from 3% to 26%. The activation of the volume-sensitive I_{Cl} channel

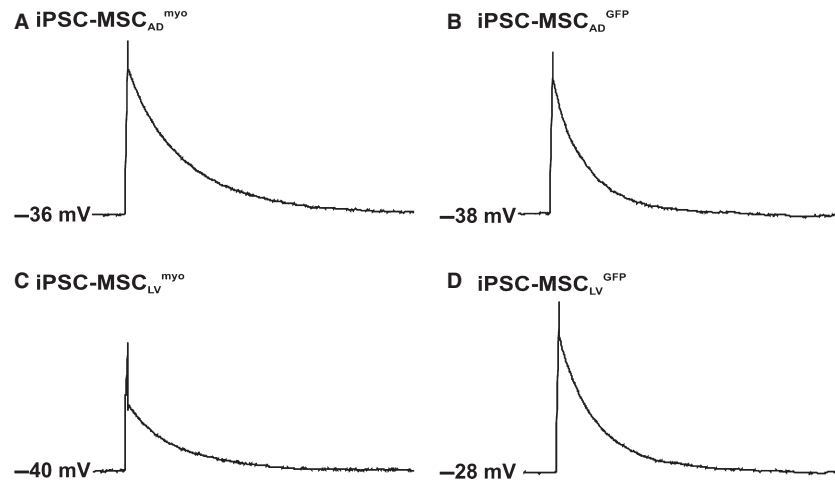


Figure 7. Action potentials in myocardin or GFP transduced iPSC-MSCs. Action potentials shown in a representative human iPSC-MSC_{AD}^{myo} (A), iPSC-MSC_{AD}^{GFP} (B), iPSC-MSC_{LV}^{myo} (C), iPSC-MSC_{LV}^{GFP} (D), iPSC-MSC_{LV}^{myo} incubated in cardiomyocyte (CM) differentiation medium for 5 days (E) or its GFP control (F).

possibly resulted from the increase in the cell volume of iPSC-MSC_{LV}^{myo}.

The I_{to} channel is encoded by Kv1.4, Kv4.2, and Kv4.3, which have been detected in the human heart (Gaborit et al. 2007). In this study, the expression of Kv4.3, but not Kv1.4 and Kv4.2, was found in iPSC-MSC_{LV}^{myo}. Therefore, the I_{to} current recorded in iPSC-MSC_{LV}^{myo} is likely mediated by the expression of Kv4.3. The I_{to} current is one of the critical components of the action potential in mature ventricular cardiomyocytes (Amin et al. 2010). 4-AP sensitive I_{to} current has been observed in atrial and ventricular cardiomyocytes (Li et al. 1995, 1998). In this study, I_{to} current has been detected in only 4% of iPSC-MSC_{LV}^{myo}. These results suggest that overexpression of myocardin directs the transdifferentiation of iPSC-MSCs to cardiomyocyte phenotypes, although at a very low efficiency.

In addition, myocardin can activate the expression of SMC marker genes in mouse ESCs (Du et al. 2003), fibroblast (Wang and Wang 2003), human BM-MSCs and fibroblast (van Tuyn et al. 2005), and human ventricular scar fibroblast (van Tuyn 2003). In this study, myocardin induced the expression of SMC marker genes (i.e., SM22, MYH11, calponin, and SM α -actin) in the iPSC-MSCs. However, myocardin expression did not induce complete SMC transdifferentiation (Yoshida et al. 2004). Although the potential role of SMC transdifferentiation remains unclear, MSC-derived SMC might enhance vasculogenesis.

The expression of SCN9A mRNA is significantly upregulated in iPSC-MSC_{LV}^{myo} compared with that in iPSC-MSC_{LV}^{GFP} or non-transduced cells. SCN9A might be responsible for the $I_{Na,TTX}$ current recorded in

iPSC-MSC_{LV}^{myo} (4%). The $I_{Na,TTX}$ current has been observed in the human BM-MSCs (Li et al. 2005) and cardiac fibroblasts (Li et al. 2009). However, no TTX-resistant sodium current encoded by SCN5A has been recorded in the iPSC-MSC_{LV}^{myo}. The expression level of SCN5A is much higher than that of SCN9A in the human heart (Gaborit et al. 2007). Furthermore, other important ion currents, such as $I_{Ca,L}$ and I_f that compose the action potential of cardiomyocytes (Amin et al. 2010) have not been detected in iPSC-MSC_{LV}^{myo}. These data again suggest that myocardin induces incomplete cardiomyocyte transdifferentiation from iPSC-MSCs.

In addition to the induction of the functional expression of the I_{to} and $I_{Na,TTX}$ channels, forced myocardin expression interferes with the expression of the IK_{Ca} and the ether à go-go 1 potassium (responsible for IK_{DR}) channels. The occurrence of the IK_{Ca} current (possibly encoded by the KCa3.1) in iPSC-MSC_{LV}^{GFP} is approximately 6%, which is comparable with those in iPSC-MSCs (5%, (Zhang et al. 2012)). The absence of the IK_{Ca} current in iPSC-MSC_{LV}^{myo} might have resulted from the decreased expression of KCa3.1. As we have shown previously, the ether à go-go 1 potassium channel is critical in the regulation of the proliferation of iPSC-MSCs (Zhang et al. 2012). The proliferation of iPSC-MSC_{LV}^{myo} has been greatly suppressed (data not shown). Myocardin possibly downregulates the expression of the ether à go-go 1 potassium channel and thus inhibits the proliferation of iPSC-MSC_{LV}^{myo}.

With a conduction gap in an NRVM-seeded MEA plate filled with desired cells, Pijnappels et al. (2006) measured the conduction velocities of BM-MSCs and NRVMs to be

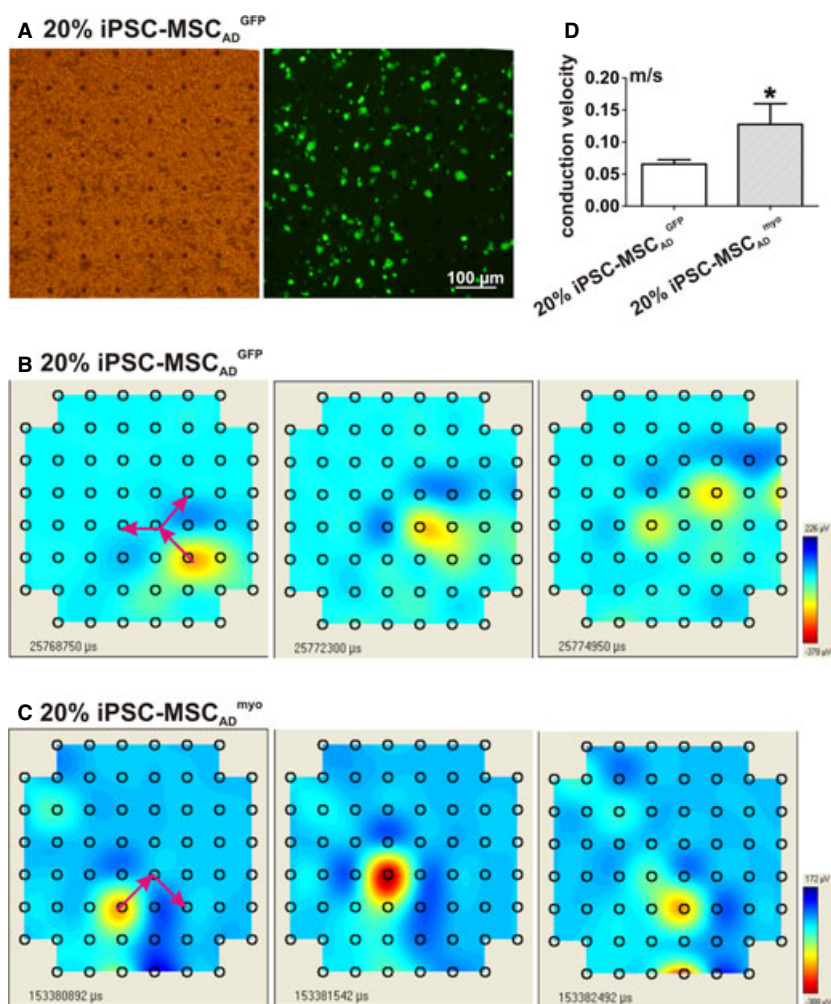


Figure 8. Cocultures of NRVMs and iPSC-MSC. (A) NRVMs were cocultured with iPSC-MSC_{AD}^{GFP} on a MEA recording plate. The electrical signals transmitted through MEA plate were recorded in NRVMs cocultured with 20% iPSC-MSC_{AD}^{GFP} (B), or iPSC-MSC_{AD}^{myo} (C), with the average conduction velocity of 0.07 ± 0.01 m/sec and 0.13 ± 0.03 m/sec, respectively (D). * $P < 0.05$.

0.014 ± 0.004 m/sec and 0.168 ± 0.002 m/sec, respectively. Moreover, they have demonstrated that the electrical conduction of BM-MSCs is caused by the expression of Cx43. Subsequently, they further showed that the forced myocardin expression induces the human ventricular scar fibroblasts to repair the conduction block of the NRVM field, possibly mediated by the upregulation of the expression of Cx40 and Cx45 (van Tuyn 2003). In contrast to these observations, our results showed that Cx40 and Cx45 expression, but not Cx43 were reduced upon myocardin transduction. While Cx40 and Cx45 are expressed in the embryonic heart, their expressions in the adult heart are mainly localized to pacemaker and conduction system. On the other hand, Cx43 is abundantly expressed in the myocardium. Therefore, downregulation of Cx40 and Cx45 after myocardin transduction

may represent a transdifferentiation to a more mature ventricular phenotype (Verheule and Kaese 2013). Nevertheless, the conduction velocity of NRVMs cocultured iPSC-MSC_{AD}^{myo} was significantly faster than that of their GFP counterparts. Therefore, forced myocardin expression increased conduction velocity possibly because of its effects on the ion channel expression of iPSC-MSCs rather than changes in connexins expression, in particular, by activating the expression of INa. TTX. Moreover, this increase in conduction velocity might account for the superior therapeutic potential of myocardin transduced BM-MSCs than that of BM-MSCs themselves in the mouse model of myocardial infarction (Grauss et al. 2008). These results suggest that similar to BM-MSCs, iPSC-MSCs are capable of conducting the electrical signals from NRVMs. More importantly, forced myocardin

expression enhances the electrical conduction of iPSC-MSCs.

The forced myocardin expression in human iPSC-MSCs lead to partial transdifferentiation into cardiomyocytes and SMC phenotypes, modified the expression profile of the ion channels, and improved the electrical conduction velocity during coculturing with NRVM. The changes in the electrophysiological properties of iPSC-MSC can potentially improve their electrical coupling with native cardiomyocytes after transplantation, thus reducing the risk of proarrhythmias. However, the therapeutic effect of the ectopic expression of myocardin in iPSC-MSCs for cardiac repair and regeneration warrants further investigation in in vivo animal models of cardiac injuries such as myocardial infarction.

Conflict of Interest

None declared.

References

- Amin, A. S., H. L. Tan, and A. A. M. Wilde. 2010. Cardiac ion channels in health and disease. *Heart Rhythm* 7:117–126.
- Borsani, G., E. I. Rugarli, M. Tagliatela, C. Wong, and A. Ballabio. 1995. Characterization of a human and murine gene (*clcn3*) sharing similarities to voltage-gated chloride channels and to a yeast integral membrane protein. *Genomics* 27:131–141.
- Chen, J. F., S. Wang, Q. Wu, D. Cao, T. Nguyen, Y. Chen, et al. 2008. Myocardin marks the earliest cardiac gene expression and plays an important role in heart development. *Anat. Rec. (Hoboken)* 291:1200–1211.
- Deng, X. L., H. Y. Sun, C. P. Lau, and G. R. Li. 2006. Properties of ion channels in rabbit mesenchymal stem cells from bone marrow. *Biochem. Biophys. Res. Commun.* 348:301–309.
- Du, K. L., H. S. Ip, J. Li, M. Chen, F. Dandre, W. Yu, et al. 2003. Myocardin is a critical serum response factor cofactor in the transcriptional program regulating smooth muscle cell differentiation. *Mol. Cell. Biol.* 23:2425–2437.
- Gaborit, N., S. Le Bouter, V. Szuts, A. Varro, D. Escande, S. Nattel, et al. 2007. Regional and tissue specific transcript signatures of ion channel genes in the non-diseased human heart. *J. Physiol.* 582:675–693.
- Grauss, R. W., J. van Tuyn, P. Steendijk, E. M. Winter, D. A. Pijnappels, B. Hogers, et al. 2008. Forced myocardin expression enhances the therapeutic effect of human mesenchymal stem cells after transplantation in ischemic mouse hearts. *Stem Cells* 26:1083–1093.
- Hoofnagle, M. H., R. L. Nepl, E. L. Berzin, G. C. Teg Pipes, E. N. Olson, B. W. Wamhoff, et al. 2011. Myocardin is differentially required for the development of smooth muscle cells and cardiomyocytes. *Am. J. Physiol. Heart Circ. Physiol.* 300:H1707–H1721.
- Huang, J., M. Min Lu, L. Cheng, L. J. Yuan, X. Zhu, A. L. Stout, et al. 2009. Myocardin is required for cardiomyocyte survival and maintenance of heart function. *Proc. Natl. Acad. Sci. USA* 106:18734–18739.
- Jin, N. G., J. K. Kim, D. K. Yang, S. J. Cho, J. M. Kim, E. J. Koh, et al. 2003. Fundamental role of *clc-3* in volume-sensitive Cl^- channel function and cell volume regulation in AGS cells. *Am. J. Physiol. Gastrointest. Liver Physiol.* 285:G938–G948.
- Lee, Y. K., K. M. Ng, W. H. Lai, Y. C. Chan, Y. M. Lau, Q. Lian, et al. 2011. Calcium homeostasis in human induced pluripotent stem cell-derived cardiomyocytes. *Stem Cell Rev.* 7:976–986.
- Li, G. R., J. Feng, Z. Wang, B. Fermini, and S. Nattel. 1995. Comparative mechanisms of 4-aminopyridine-resistant Ito in human and rabbit atrial myocytes. *Am. J. Physiol.* 269: H463–H472.
- Li, G. R., J. Feng, L. Yue, and M. Carrier. 1998. Transmural heterogeneity of action potentials and Ito1 in myocytes isolated from the human right ventricle. *Am. J. Physiol.* 275: H369–H377.
- Li, G. R., H. Sun, X. Deng, and C. P. Lau. 2005. Characterization of ionic currents in human mesenchymal stem cells from bone marrow. *Stem Cells* 23:371–382.
- Li, G. R., H. Y. Sun, J. B. Chen, Y. Zhou, H. F. Tse, and C. P. Lau. 2009. Characterization of multiple ion channels in cultured human cardiac fibroblasts. *PLoS One* 4:e7307.
- Lian, Q., Y. Zhang, J. Zhang, H. K. Zhang, X. Wu, Y. Zhang, et al. 2010. Functional mesenchymal stem cells derived from human induced pluripotent stem cells attenuate limb ischemia in mice. *Circulation* 121:1113–1123.
- Pijnappels, D. A., M. J. Schali, J. van Tuyn, D. L. Ypey, A. A. de Vries, E. E. van der Wall, et al. 2006. Progressive increase in conduction velocity across human mesenchymal stem cells is mediated by enhanced electrical coupling. *Cardiovasc. Res.* 72:282–291.
- Siu, C. W., and H. F. Tse. 2012. Cardiac regeneration: messages from caduceus. *Lancet* 379:870–871.
- Small, E. M., A. S. Warkman, D. Z. Wang, L. B. Sutherland, E. N. Olson, and P. A. Krieg. 2005. Myocardin is sufficient and necessary for cardiac gene expression in xenopus. *Development* 132:987–997.
- Tao, R., C. P. Lau, H. F. Tse, and G. R. Li. 2007. Functional ion channels in mouse bone marrow mesenchymal stem cells. *Am. J. Physiol. Cell Physiol.* 293:1561–1567.
- Torrado, M., E. López, A. Centeno, C. Medrano, A. Castro-Beiras, and A. T. Mikhailov. 2003. Myocardin mRNA is augmented in the failing myocardium: expression profiling in the porcine model and human dilated cardiomyopathy. *J. Mol. Med.* 81:566–577.

- van Tuyn, J., D. A. Pijnappels, A. A. de Vries, I. de Vries, I. van der Velde-van Dijke, S. Knaän-Shanzer, et al. 2003. Fibroblasts from human postmyocardial infarction scars acquire properties of cardiomyocytes after transduction with a recombinant myocardin gene. *FASEB J.* 21:3369–3379.
- van Tuyn, J., S. Knaän-Shanzer, M. J. van de Watering, M. de Graaf, A. van der Laarse, M. J. Schalij, et al. 2005. Activation of cardiac and smooth muscle-specific genes in primary human cells after forced expression of human myocardin. *Cardiovasc. Res.* 67:245–255.
- Verheule, S., and S. Kaese. 2013. Connexin diversity in the heart: insights from transgenic mouse models. *Front. Pharmacol.* 4:81.
- Wang, Z., D. Z. Wang, G. C. Teg Pipes, and E. N. Olson. 2003. Myocardin is a master regulator of smooth muscle gene expression. *Proc. Natl. Acad. Sci. USA* 100:7129–7134.
- Wang, L., L. Chen, and T. J. C. Jacob. 2000. The role of clc-3 in volume-activated chloride currents and volume regulation in bovine epithelial cells demonstrated by antisense inhibition. *J. Physiol.* 524:63–75.
- Wang, D., P. S. Chang, Z. Wang, L. Sutherland, J. A. Richardson, E. Small, et al. 2001. Activation of cardiac gene expression by myocardin, a transcriptional cofactor for serum response factor. *Cell* 105:851–862.
- Williams, A. R., and J. M. Hare. 2011. Mesenchymal stem cells: biology, pathophysiology, translational findings, and therapeutic implications for cardiac disease. *Circ. Res.* 109:923–940.
- Xiong, D., N. S. Heyman, J. Airey, M. Zhang, C. A. Singer, S. Rawat, et al. 2010. Cardiac-specific, inducible clc-3 gene deletion eliminates native volume-sensitive chloride channels and produces myocardial hypertrophy in adult mice. *J. Mol. Cell. Cardiol.* 48:211–219.
- Yoshida, T., S. Sinha, F. Dandré, B. R. Wamhoff, M. H. Hoofnagle, B. E. Kremer, et al. 2003. Myocardin is a key regulator of CArG-dependent transcription of multiple smooth muscle marker genes. *Circ. Res.* 92:856–864.
- Yoshida, T., K. Kawai-Kowase, and G. K. Owens. 2004. Forced expression of myocardin is not sufficient for induction of smooth muscle differentiation in multipotential embryonic cells. *Arterioscler. Thromb. Vasc. Biol.* 24:1596–1601.
- Zhang, J., Y. C. Chan, J. C. Ho, C. W. Siu, Q. Lian, and H. F. Tse. 2012. Regulation of cell proliferation of human induced pluripotent stem cell-derived mesenchymal stem cells via ether a go-go 1 (hEAG1) potassium channel. *Am. J. Physiol. Cell Physiol.* 303:C115–C125.